Electron acceleration by a propagating laser pulse in low-density plasma

Fengchao Wang (王凤超), Baifei Shen (沈百飞), Xiaomei Zhang (张晓梅), Xuemei Li (李雪梅), and Zhangying Jin (金张英)

State Key Laboratory of High Field Laser Physics, Shanghai Institute of Optics and Fine Mechanics, Chinese Academy of Sciences, Shanghai 201800

Electron acceleration by a propagating short ultra-intense laser pulse in a low-density plasma has been investigated. Electrons have the maximum energy when meeting the peak of the laser pulse. If a propagating laser pulse is abruptly stopped by a solid target, the highly energetic electrons will continue to move forward inertially and escape from the laser field. The envelope of the laser pulse is taken into account and there is an optimal position between the electron and the solid target. The electron maximum energy depends on the laser intensity and initial electron energy, and has nothing to do with the polarization of the pulse, but a linearly polarized laser pulse is more effective to accelerate electron than circularly polarized one under the same laser energy. The influence of the reflected light has been taken into account which makes our model more perfect and the results give good agreement with particle in cell simulations.

OCIS codes: 140.7090, 350.5400, 350.5720, 260.2160.

Based on the chirped-pulse amplification technique, ultrahigh and ultrashort laser has been rapidly developed. This has stimulated many new research areas about laser-plasma interaction, such as laser-driven nuclear[1], particle acceleration. Among these, laser acceleration of electrons has received great attention in recent years[2−7] because of the large variety of applications of high energy electrons, such as fast ignition of fusion reaction[8,9], and X-ray generation[10−12].

Two prominent approaches to laser driven electron acceleration are direct laser acceleration[13,14] and acceleration by laser driven plasma wave[15,16]. The former depends on self-generated strong azimuthal magnetic field, and the latter involves beat wave mechanism and wake field mechanism. For sufficiently short and intense laser pulse, direct electron acceleration in the pulse dominates[17]. It is known that electrons can be more efficiently accelerated by a propagating laser pulse than by a standing wave. The electron energy, scaling as the laser intensity I at the peak of the propagating pulse, can be much higher than that (scaling as $\sqrt{I}$) from a standing wave pulse[18]. How to extract the energetic electrons from the laser pulse is a very important issue. It is well known that a planar-wave cannot be used for electron acceleration, since the pondermotive force pushes an electron forward in the ascending front and pulls an electron backward in the descending part of the laser pulse when a wave overtakes the electron. So electrons have the maximum energy when they meet the peak of the laser pulse. If the propagating laser pulse is abruptly stopped by a solid target, the highly energetic electrons will continue to move forward inertially and escape from the laser field as well as the target without much energy loss if their stopping distance is much larger than the laser skin depth and the target thickness, respectively. Yu *et al.*[19] have researched this proposed acceleration and extraction processes by particle in cell (PIC) simulations, and given out the electron maximum energy by using well-known analytic solution for relativistic electron motion in a plane electromagnetic wave propagating in vacuum. An analytical model has been presented in Ref. [20], the author adopted the constant amplitude laser pulse and discussed the relationship of the maximum energy and the phase of the laser wave.

In this paper, the envelope of laser pulse is taken into account, so it is difficult to ascertain the optimal position of the solid target where the electron gains the maximum energy. This problem is solved very well in our model, we adopt a Gaussian laser pulse and introduce the position of the target z_1 in the expression of the reflected wave, so we can easily find the optimal position of the target by changing z_1. In this scheme a very low density preplasma is produced at the front of the solid target to supply electrons to be accelerated. It is known that if the density of the preplasman is low relatively to the critical density n_c, $n/n_c < 0.02$, the instability of plasma can be neglected, and the light propagation as well as the electron dynamics in the low density preplasma are approximated by that in a vacuum.

We consider the propagation of a laser pulse with vector potentials,

$$\vec{A} = A_0 \exp\{-[t-(z-z_0)/c]^2/\tau^2\} \times[\hat{x}\cos(\omega t - kz) + \beta\hat{y}\sin(\omega t - kz)], \quad (1)$$

where A_0 is the maximum amplitude of laser pulse, z_0 is the initial position of pulse peak, z_1 is the position of the target, ω is the frequency of laser, k is wave vector, τ is the pulse duration, c is the light velocity in vacuum, and $\beta = 1$ and $\beta = 0$ correspond to circularly and linearly polarized laser pulse, respectively. Based on the ideal conductor model, the reflected wave can be expressed as

$$\vec{A'} = A_0 \exp\{-[t+[z-(2z_1-z_0)]/c]^2/\tau^2\} \times[-\hat{x}\cos(\omega t + k(z-2z_1)) -\beta\hat{y}\sin(\omega t + k(z-2z_1))]. \quad (2)$$

The electromagnetic fields related to the vector potential of the laser pulse are

$$\vec{E} = -\frac{\partial \vec{A}}{\partial t} \quad \text{and} \quad \vec{B} = \bigtriangledown \times \vec{A}. \quad (3)$$

The equations governing electron momentum and energy

are

$$\frac{\mathrm{d}p_x}{\mathrm{d}t} = e\frac{\partial(A_x + A'_x)}{\partial t} + ev_z\frac{\partial(A_x + A'_x)}{\partial z}, \quad (4)$$

$$\frac{\mathrm{d}p_y}{\mathrm{d}t} = e\frac{\partial(A_y + A'_y)}{\partial t} + ev_z\frac{\partial(A_y + A'_y)}{\partial z}, \quad (5)$$

$$\frac{\mathrm{d}p_z}{\mathrm{d}t} = -ev_x\frac{\partial(A_x + A'_x)}{\partial z} - ev_y\frac{\partial(A_y + A'_y)}{\partial z}, \quad (6)$$

$$\frac{\mathrm{d}(\gamma m_0 c^2)}{\mathrm{d}t} = ev_x\frac{\partial(A_x + A'_x)}{\partial t} + ev_y\frac{\partial(A_y + A'_y)}{\partial t}, \quad (7)$$

where $-e$ and m_0 are electron charge and rest mass, respectively. The integration of Eqs. (6) and (7) yields

$$\frac{\mathrm{d}}{\mathrm{d}t}(p_z - \gamma m_0 c) = 0,$$
$$p_z - \gamma m_0 c = C_1, \quad (8)$$

where C_1 is given by initial conditions. If the electron is with $p_x = 0$ and $p_y = 0$ initially and $\gamma = \gamma_0$, then $C_1 = [(\gamma_0^2 - 1)^{1/2} - \gamma_0]m_0 c$.

In the following discussion, the following dimensionless variables will be used,

$$a_0 \to \frac{eA_0}{m_0 c}, \quad t \to \frac{t}{T}, \quad \tau \to \frac{\tau}{T}, \quad x \to \frac{x}{\lambda},$$
$$y \to \frac{y}{\lambda}, \quad z \to \frac{z}{\lambda}, \quad \frac{\mathrm{d}x}{\mathrm{d}t} \to (\mathrm{d}x/\mathrm{d}t)/c,$$
$$\frac{\mathrm{d}y}{\mathrm{d}t} \to (\mathrm{d}y/\mathrm{d}t)/c, \quad \frac{\mathrm{d}z}{\mathrm{d}t} \to (\mathrm{d}z/\mathrm{d}t)/c.$$

In these variables, Eq. (4)-(8) can be rewritten as

$$\frac{\mathrm{d}x}{\mathrm{d}t} = \frac{1}{\gamma}(a_x + a'_x), \quad (9)$$

$$\frac{\mathrm{d}y}{\mathrm{d}t} = \frac{1}{\gamma}(a_y + a'_y), \quad (10)$$

$$\frac{\mathrm{d}z}{\mathrm{d}t} = \frac{1}{\gamma}[(\gamma_0 - 1)^{1/2} - \gamma_0 + \gamma], \quad (11)$$

$$\begin{aligned}\frac{\mathrm{d}\gamma}{\mathrm{d}t} = &-\frac{1}{\gamma}\frac{\mathrm{d}x}{\mathrm{d}t}\{2\pi a_y + 2a_x[t - (z - z_0)]/\tau^2 \\ &+2\pi a'_y + 2a'_x[t + (z - (2z_1 - z_0))]/\tau^2\} \\ &+\frac{1}{\gamma}\frac{\mathrm{d}y}{\mathrm{d}t}\{2\pi a_x + 2a_y[t - (z - z_0)]/\tau^2 \\ &+2\pi a'_x + 2a'_y[t + (z - (2z_1 - z_0))]/\tau^2\}. \quad (12)\end{aligned}$$

where

$$\begin{aligned}a_x &= a_0 \exp\{-[t - (z - z_0)]/\tau^2\}\cos[2\pi(t - z)], \\ a'_x &= -a_0 \exp\{-[t + (z - (2z_1 - z_0))]/\tau^2\} \\ &\quad \times \cos[2\pi(t + (z - 2z_1))], \\ a_y &= \beta a_0 \exp\{-[t - (z - z_0)]/\tau^2\}\sin[2\pi(t - z)], \\ a'_y &= -\beta a_0 \exp\{-[t + (z - (2z_1 - z_0))]/\tau^2\} \\ &\quad \times \sin[2\pi(t + (z - 2z_1))].\end{aligned}$$

Equations (9)−(12) are coupled ordinary differential equations, which have been solved numerically by the fourth order Runge-Kutta method for electron energy for different positions, different laser intensities, and different initial energy γ_0.

The results are presented in the form of dimensionless variables, and the energy loss during electron passing through the target has been neglected. We have chosen $\tau = 7$ and $z_0 = -20$.

Figure 1 shows the electron energy γ as a function of z for $a_0 = 7.5$ and $\gamma_0 = 1$ with linearly and circularly polarized laser pulse, respectively. It shows that electrons can not gain net energy at last if there is no target to stop the laser pulse. But if we put a target at the optimal positions $z_1 = 61.78$ for linearly polarized and $z_1 = 125$ for circularly polarized laser pulse, it can be seen from Fig. 1 (b) that electrons accelerated by a linearly and circularly polarized laser pulse have the same maximum energy $\gamma \simeq 29$. The linearly polarized laser pulse is more effective to accelerate electron than circularly polarized one, because the intensity of linearly polarized laser is only the half of the circularly one with the same amplitude a_0. Near the target, due to the influence of the reflected laser pulse, the energy of the electron shows irregular change, especially for linearly polarized laser pulse.

When the position of target is fixed, electrons on different initial positions gain different energy, as shown in Fig. 2. Figures 2(a) and (b) show the results of a linearly and circularly polarized laser pulse, respectively, at $a_0 = 7.5$ and $\gamma_0 = 1$. It is obvious that both the linearly and circularly polarized laser pulses have their optimal acceleration length, so there is an optimal initial position between the electron and the solid target. Concretely, the initially stationary electron at $z_r = 61.78$ and $z_r = 125$ for linearly and circularly polarized laser pulses gains the biggest energy. If the electron is far away from the optimal position, there is nearly no energy gain after the interaction. The optimal position is different

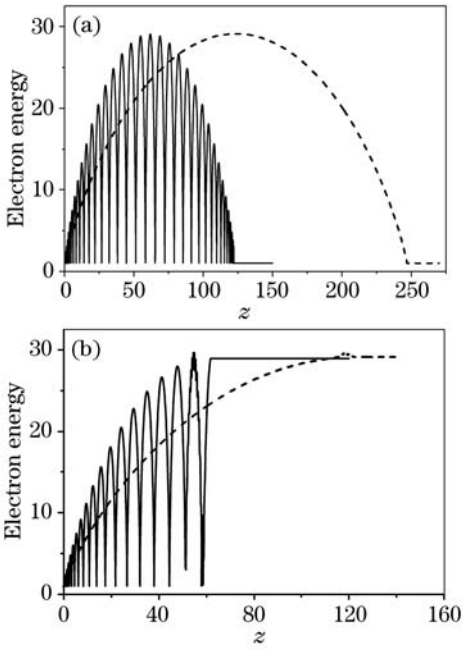

Fig. 1. Electron energy γ as a function of z at $a_0 = 7.5$ and $\gamma_0 = 1$ for linearly (solid lines) and circularly polarized laser pulses (dashed lines), respectively. (a) With no target, (b) the position of the target at $z_1 = 61.78$ for linearly polarized and $z_1 = 125$ for circularly polarized laser pulses.

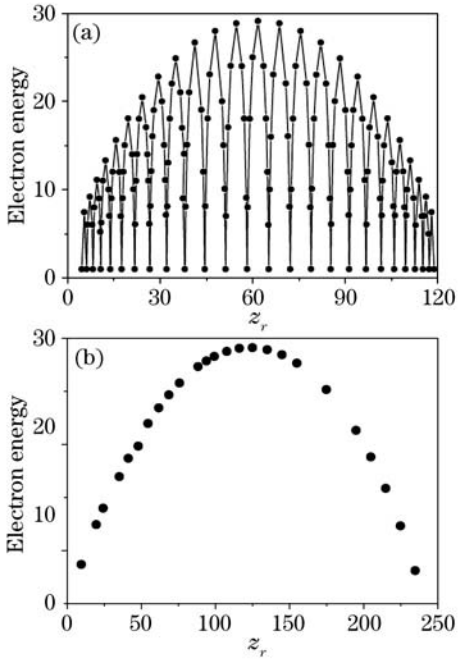

Fig. 2. Dependence of electron energy gain on the relative distance between the initial position of electron and the target z_r at $a_0 = 7.5$ and $\gamma_0 = 1$. (a) Linearly polarized laser pulse; (b) circularly polarized laser pulse.

for different parameters, which can be easily ascertained by our model.

We have investigated the acceleration process in Figs. 3 and 4. We consider a linearly (or circularly) polarized laser pulse with dimensionless amplitude $a_0 = 7.5$, wavelength $\lambda = 1$ μm, and pulse duration $L = 15\lambda$ normally incident on the preplasma of width $d = 0.1\lambda$ and density $n = 0.05n_c$. The initial position of the left boundary of preplasma is $z = 20\lambda$. Because of the width the preplasma is so narrow in comparison with the acceleration distance we can assume all the electrons at the same position. Figures 3(a) and 4(a) show the electron density distribution at $t = 40T$ and $t = 80T$ for the linearly and circularly polarized laser pulse, respectively, where $T = \lambda/c$. It can be seen that almost all electrons centralize to two parts in the circularly polarize laser field and the electron density of one part is higher than initial, and in the linearly polarized laser pulse field, although there are two high density parts, both of them are lower than initial electron density, and there are a lot of electrons between the two parts. Figures 3(b) and 4(b) show the electron energy spectrum at $t = 40T$ and $t = 80T$ for linearly and circularly polarized laser pulse, respectively. It can be seen that there are also two parts in the energy spectrum corresponding to the density distribution for circularly polarized laser, and for every part electrons almost have the same energy. For linearly polarized laser, the electron energy spectrum is wide (from 1 to 18), it mainly because the electron energy is oscillatory in a linearly polarized laser field.

Figure 5 shows the longitudinal electron momentum spectra at $t = 82T$ and $t = 88T$. The preplasma's width $d = 60$ μm and density $n = 0.005n_c$, and its initial position of the left boundary is $z = 20\lambda$, the solid target's thickness and density are 8λ and $10n_c$, and its left boundary is at $z = 80\lambda$. The linearly polarized laser pulses parameters are the same as Figs. 3 and 4. It can be seen from Fig. 5(a) that the longitudinal forward momentum distribution is in good agreement with the analytical results. When electrons are only accelerated by laser pulse, the maximum electron momentum is $p_z \simeq 28$. Figure 5(b) shows the results after the pulse center arrives at the target, because of the influence of the target's electric field, some electrons gains more energy. Of cause, electron movement is also affected by the electric field in the plasma. There are maximum values

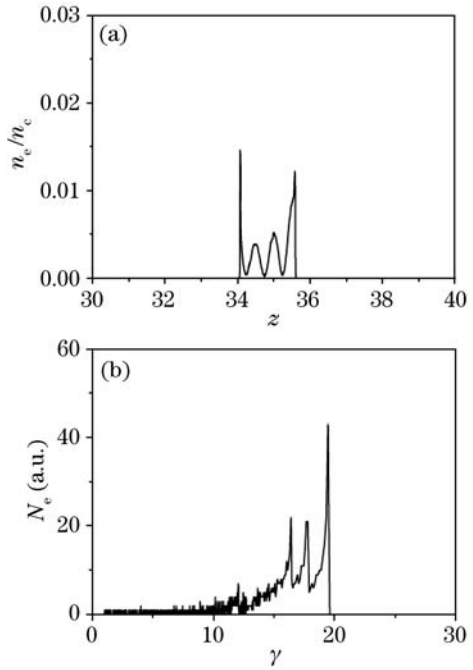

Fig. 3. (a) Electron density distribution and (b) electron energy spectrum at $t = 40T$ for linearly polarized laser pulse.

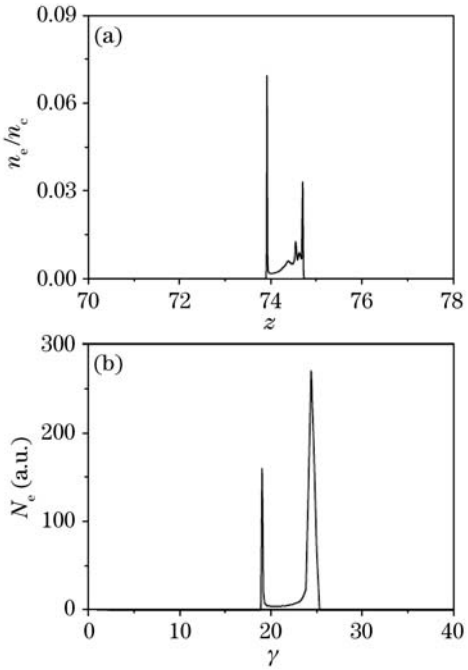

Fig. 4. (a) Electron density distribution and (b) electron energy spectrum at $t = 80T$ for circularly polarized laser pulse.

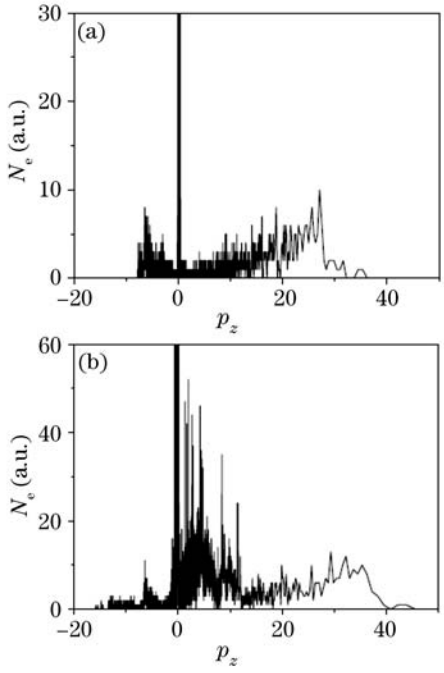

Fig. 5. Longitudinal electron momentum spectra for a linearly polarized laser pulse. (a) $t = 82T$; (b) $t = 88T$.

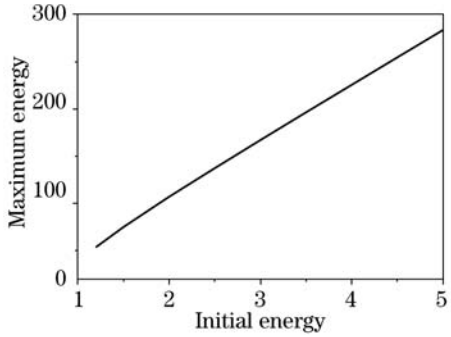

Fig. 6. Maximum energy $\gamma_{\max}$ as a function of the initial energy γ_0 for circularly polarized laser pulse with amplitude $a_0 = 7.5$.

at $p_z = 0$ in Figs. 5(a) and (b), because a lot of target's electrons don't move. Because of the electric field and the backward pondermotive force, electrons which behind the laser pulse will move backward.

Figure 6 shows the maximum energy $\gamma_{\max}$ as a function of the initial energy γ_0 for a circularly polarized laser pulse at $a = 7.5$. The Maximum energy $\gamma_{\max}$ increases with initial energy γ_0 linearly. It shows that the initial energy γ_0 plays a very important role for the final energy of electrons. We have the same result if the laser is linearly polarized.

In conclusion, we have studied electrons acceleration by a propagating short ultraintense laser pulse in a low-density plasma in front of a solid target. The envelope of the laser pulse is taken into account. Electrons gain the maximum energy when they meet the peak of the laser pulse. If the electrons are rest initially, the maximum energy is proportional to a_0^2 ($\gamma_{\max} = a_0^2/2 + 1$). If the initial energy $\gamma_0 > 1$, the maximum energy increases rapidly with the initial energy linearly, so the initial energy as well as laser intensity plays an important role in energy gain. The linearly polarized laser pulse is more effective to transfer its energy to electron than circularly polarized one under the same laser energy. The target position is another important issue to the final energy in addition to the laser density and the initial energy. Both linearly and circularly polarized laser pulses have their optimal acceleration length, so there is an optimal initial position where an electron gains maximum energy. The optimal positions of target are different for different parameters.

This work was supported by the National Natural Science Foundation of China under Grant No. 10675155. F. Wang's e-mail address is fchwang@siom.ac.cn.

References

1. B. Shen, X. Zhang, and M. Y. Yu, Phys. Rev. E **71,** 015401 (2005).
2. F. He, W. Yu, P. Lu, H. Xu, L. Qian, B. Shen, X. Yuan, R. Li, and Z. Xu, Phys. Rev. E **68,** 046407 (2003).
3. K. P. Singh, Phys. Rev. E **69,** 056410 (2004).
4. D. N. Gupta and C. Ryu, Phys. Plasmas **12,** 053103 (2005).
5. P. Sprangle, E. Esarey, and J. Krall, Phys. Plasmas **3,** 2183 (1996).
6. K. P. Singh, Appl. Phys. Lett. **87,** 254102 (2005).
7. V. V. Kulagin, V. A. Cherepenin, and H. Suk, Phys. Plasmas **11,** 5239 (2004).
8. M. Tabak, J. Hammer, M. E. Ginsky, W. L. Kruer, S. C. Wilks, J. Woodworth, E. M. Campbell, and M. D. Perry, Phys. Plasmas **1,** 1626 (1994).
9. C. Ren, M. Tzoufras, J. Tonge, W. B. Mori, F. S. Tsung, M. Fiore, R. A. Fonseca, L. O. Silva, J. C. Adam, and A. Heron, Phys. Plasmas **13,** 056308 (2006).
10. S. Fritzler, K. Ta phuoe, V. Malka, A. Rousse, and E. Lefebvre, Appl. Phys. Lett. **83,** 3888 (2003).
11. Y. Sentoku, K. Mima, T. Taguchi, S. Miyamoto, and Y. Kishimoto, Phys. Plasmas **5,** 4366 (1998).
12. N. Hafz, H. J. Lee, G. H. Kim, J. U. Kim, H. Suk, and J. Lee, IEEE Trans. Plasma Sci. **31,** 1388 (2003).
13. G. D. Tsakiris, C. Gahn, and V. K. Tripathi, Phys. Plasmas **7,** 3017 (2000).
14. C. Gahn, G. D. Tsakiris, A. Pukhov, J. Meyer-ter-Vehn, G. Pretzler, P. Thirolf, D. Habs, and K. Witte, Phys. Rev. Lett. **83,** 4772 (1999).
15. R. Wagner, S. Y. Chen, A. Maksimchuk, and D. Umstadter, Phys. Rev. Lett. **78,** 3125 (1997).
16. W. P. Leemans, P. Catravas, E. Esarey, C. G. R. Geddes, C. Toth, R. Trines, C. B. Schroeder, B. A. Shadwick, J. V. Tilborg, and J. Faure, Phys. Rev. Lett. **89,** 174802 (2002).
17. M. Y. Yu, W. Yu, Z. Y. Chen, J. Zhang, Y. Yin, L. H. Cao, P. X. Lu, and Z. Z. Xu, Phys. Plasmas **10,** 2468 (2003).
18. S. C. Wilks, W. L. Kruer, M. Tabak, and A. B. Langdon, Phys. Rev. Lett. **69,** 1383 (1992).
19. W. Yu, V. Bychenkov, Y. Sentoku, M. Y. Yu, Z. M. Sheng, and K. Mima, Phys. Rev. Lett. **85,** 570 (2000).
20. K. P. Singh, Phys. Plasmas **11,** 1164 (2004).